Available online at www.sciencedirect.com
ScienceDirect
Journal of Solid State Chemistry 179 (2006) 3252–3259
JOURNAL OF SOLID STATE CHEMISTRY
www.elsevier.com/locate/jssc

Rapid communication

Thermal characteristics, Raman spectra and structural properties of new tellurite glasses within the Bi_2O_3–TiO_2–TeO_2 system

M. Udovic[a,b], P. Thomas[a,*], A. Mirgorodsky[a], O. Durand[a], M. Soulis[a], O. Masson[a], T. Merle-Méjean[a], J.C. Champarnaud-Mesjard[a]

[a]*Science des Procédés Céramiques et de Traitements de Surface, UMR 6638 CNRS, Faculté des Sciences et Techniques, 123 Avenue Albert Thomas, 87060 Limoges Cedex, France*
[b]*Jozef Stefan Institute, Jamova 39, 1000 Ljubljana, Slovenia*

Received 20 March 2006; received in revised form 29 May 2006; accepted 18 June 2006
Available online 21 June 2006

Abstract

Within the Bi_2O_3–XO_2–TeO_2 (X = Ti, Zr) systems, a large glass-forming domain was found for X = Ti, but no glass formation was evidenced for X = Zr. Densities, glass transition (T_g), crystallization (T_c) temperatures and Raman spectra of the relevant glasses were studied as functions of the composition. The Raman spectra of the glasses were interpreted in terms of the structural transformations produced by the modifiers. It was established that the addition of Bi_2O_3 and TiO_2 content to TeO_2 glass influences the T_g temperature in a similar manner: this value progressively increases with the increase of the modifier concentration. However, the structural evolutions are different: (a) the addition of TiO_2 to TeO_2 glass keeps the polymerized framework structure in transforming a number of Te–O–Te bridges into the Te–O–Ti ones without producing any tellurite anions (i.e., the $[TeO_3]^{2-}$ groups); (b) on the contrary, the addition of Bi_2O_3 destroys the glass framework by giving rise to the island-type $[Te_nO_m]^{2(m-2n)-}$ complex tellurites anions, thus causing a depolymerization of the glass.

Keywords: Tellurite glasses; Thermal analysis; Raman spectroscopy

1. Introduction

Increasing interest is paid during the last decade to TeO_2-based glasses for their remarkable optical properties, good thermal stability, chemical durability, broad homogeneity range and low melting temperatures (see [1] and references therein).

It should be emphasized that the non-linear optical indices of tellurium oxide-based glasses are one of the highest among oxide systems (more than one order higher than in silica and silicate glasses), which makes those materials very promising candidates for non-linear optical applications and especially for electro-optic devices [1–6].

Customarily, the origin of the extraordinary non-linear optical properties of TeO_2-based glasses is attributed to a high hyperpolarizability of a lone (i.e., localized) electron pair related to the 5*s* orbital of tellurium atom. There is a good reason to believe that the existence of such pairs is inherent in TeO_2 polymorphs and in tellurites, but strictly speaking, the extraordinary hyperpolarizability of those pairs was never evidenced. Moreover, the recent ab initio studies of $(TeO_2)_n$ clusters provide arguments to associate the above-mentioned extraordinary optic properties with the essential non-locality of the electron dielectric response, which is found to be characteristic of the $(TeO_2)_n$ chain-like polymers [7–9].

This point seems to be capable of explaining why the addition of a modifying oxide to TeO_2 glass (which is necessary to ameliorate the glass stability) decreases, as a rule, the linear and non-linear optical indices [1]. Actually, to transform this glass into a tellurite structure, the O^{2-} atoms delivered by the modifier have to react with the elementary neutral units of TeO_2 glass (which can be considered as TeO_2 molecules or, more traditionally, as $TeO_{4/2}$ disphenoids) to produce a number of the charged

*Corresponding author. Fax: +33 5 55 45 72 70.
E-mail address: philippe.thomas@unilim.fr (P. Thomas).

0022-4596/$ - see front matter © 2006 Elsevier Inc. All rights reserved.
doi:10.1016/j.jssc.2006.06.016

$[TeO_3]^{2-}$ pyramid-like units. Consequently, the initial three-dimensional TeO_2 framework would evolve into an ensemble of complex $[Te_nO_m]^{2(m-2n)-}$ tellurite anions, separated by cations [10]. As a result, the glass becomes an island-type structure, and its microscopic polarization mechanism becomes more localized, and the hyperpolarizabilty of the glass as a rule, becomes less pronounced.

However, a series of modifiers can even enhance the non-linear refractive indices of tellurite glasses [1] by virtue of a high polarizability inherent to the cations involved. Two categories of such modifiers can be mentioned. The first modifiers involve cations of heavy *p*-elements (e.g. those of the sixth period , like Tl^+, Pb^{2+} and Bi^{3+}) predisposed to form the lone electron pairs in oxides. The second involve cations of *d*-elements in which the highest orbitals are weakly occupied, e.g. W^{6+}, Nb^{5+}, Ti^{4+}, Zr^{4+}, etc.

Among the last modifiers, TiO_2 and ZrO_2 are of special interest. Actually, the X-ray diffraction patterns and the Raman spectra show that no $[TeO_3]^{2-}$ pyramids, and thus no $[Te_nO_m]^{2(m-2n)-}$ anions appear in crystalline or glassy structures within the TeO_2–TiO_2 or TeO_2–ZrO_2 systems [3,11–16] which would keep the framework nature of such compounds, thus favouring their high polarizability and hyperpolarizability.

Taking into account these points, it can be thought that ternary TeO_2-based glassy systems including TiO_2 (or ZrO_2) modifier, jointly with a modifier of the first category, can provide the glasses which would offer the best compromise on the high non-linear optical characteristics, on the one hand, and the high mechanical and thermal resistance, on the other hand. Keeping this in mind, we have performed, for the first time, the studies of the properties of the Bi_2O_3–$TiO_2(ZrO_2)$–TeO_2 systems.

Our aim was:

(i) to determine the glass formation domain;
(ii) to follow the thermal behaviour of the system: i.e. to establish their glass transition temperature (T_g), onset crystallization temperature (T_o) and temperature of the first crystallization peak (T_x);
(iii) to study the structural evolution of the glasses as a function of the composition.

2. Experimental

To obtain glassy samples (weight: ~500 mg), appropriate amounts of commercial TiO_2 (Aldrich, 99+) or ZrO_2 (Aldrich, 99+), Bi_2O_3 (Aldrich, 99.99+) and TeO_2 (prepared in the laboratory by decomposition at 550 °C for 24 h of commercial *ortho*-telluric acid H_6TeO_6 (Aldrich, 99.9%)) were first melted at 900 °C for 10 min in platinum crucibles and then air/or ice-quenched. In order to extend the glass forming range, the bottom of the platinum crucible was quickly dipped in a freezing mixture consisting of ice, ethanol and NaCl (about −14 °C). Glass formation domain was determined by using X-ray diffraction (Guinier-De Wolff camera, Cu$K\alpha_1$ radiation). The thermal behaviour of air and ice-quenched glassy samples were determined by heat flux differential scanning calorimetry DSC (Netzsch STA 409 apparatus). The powdered samples (~30 ± 1 mg) were placed into covered gold crucibles under pure flowing nitrogen atmosphere in order to prevent potential oxidation of tellurium, and the DSC curves were recorded between 20 and 800 °C using a heating rate of 10 °C/min. The glass transition temperature (T_g), onset crystallization temperature (T_o) and temperature of the first crystallization peak (T_x) were determined as indicated in Fig. 2. The densities of the glasses were measured on finely ground powders by helium pycnometry (Accupyc 1330).

A structural aspect of the glass studies was realized using Raman spectroscopy. The Raman spectra were recorded in the 80–1000 cm^{-1} range using a Jobin–Yvon spectrometer (64000 model) equipped with an Ar^+ laser (514.5 nm exciting line) and a CCD detector in a backscattering geometry. Using such a detector, a good signal/noise ratio needed two scans (during 100 s). The sample focalization was done through a microscope (× 100). The diameter of the laser spot focused on the samples was about 1 μm. Measurements were performed at low power (< 100 mW) of the excitation line, in order to avoid any damage of the glasses. The spectral resolution was about 2.5 cm^{-1} at the exciting line.

3. Results

3.1. Glass formation

Neither by air nor by ice-quenching from 900 °C any glassy phase was obtained in the Bi_2O_3–ZrO_2–TeO_2 system, or in the ZrO_2–TeO_2 system. Crystallization of the α-TeO_2 and $ZrTe_3O_8$ lattices was always identified preventing the formation of a stable glass, in line with early results [17].

Within the binary TiO_2–TeO_2 system, glasses were obtained in the range from 10 to 15 mol% of TiO_2 using air-quenching. This domain was extended in the range from 5 to 18 mol% of TiO_2 under ice-quenching conditions. The results are in perfect accordance with previous literature data [2,3] describing the glass formation in this binary system.

Practically no glass forming domain was determined within the Bi_2O_3–TeO_2 system: only a very narrow glassy compositional range (from 0 to 4 mol% of $BiO_{1.5}$) could be obtained when a small quantity of powder (about 100 mg) was melted at 900 °C and then ice-quenched. Under such conditions, a glass forming domain was evidenced up to 15 mol% of $BiO_{1.5}$ within the Bi_2O_3–TiO_2–TeO_2 system under air-quenched conditions, and was enlarged up to 25 mol% of $BiO_{1.5}$ by ice-quenching (Fig. 1).

3.2. Thermal properties and densities of glasses

The characteristics of some glasses are given in Table 1. As an illustration, the DSC curves of the $yBiO_{1.5}$–$10TiO_2$–$(90-y)TeO_2$ glasses with $0 \leqslant y \leqslant 25$ are shown in

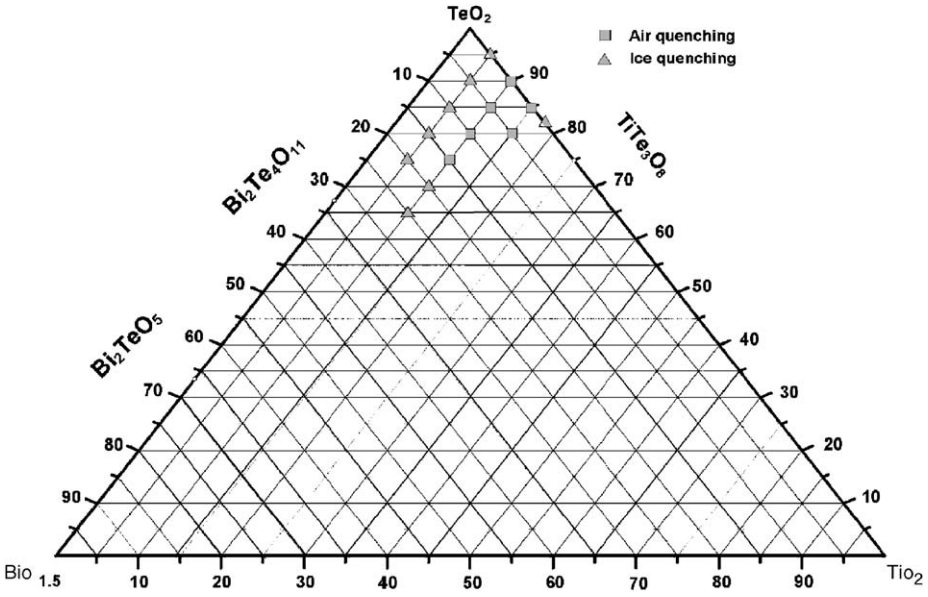

Fig. 1. Glass forming domains at 900 °C under air or ice-quenching conditions within the Bi_2O_3–TiO_2–TeO_2 system (melting time: 10 min; weight of the samples: 500 mg).

Table 1
Glass transition temperature (T_g), onset crystallization temperature (T_o), temperature of the first crystallization peak (T_x), thermal stability (T_o-T_g) and density of glasses

Mol% $BiO_{1.5}$	Mol% TiO_2	Mol% TeO_2	T_g (°C)	T_o (°C)	T_x (°C)	T_o-T_g (°C)	Density (g/cm^3)
0	5	95	313	361	368	48	5.57
0	10	90	335	397	407	62	5.47
0	15	85	356	427	441	71	5.39
0	18	82	372	446	457	74	5.33
5	5	90	321	365	375	44	5.73
5	10	85	338	425	438	87	5.66
5	15	80	362	441	450	79	5.58
10	5	85	322	361	368	39	5.94
10	10	80	341	410	429	69	5.86
15	5	80	324	352	357	28	6.13
15	10	75	347	401	416	54	6.04
20	5	75	332	357	361	25	6.30
20	10	70	351	390	397	39	6.23
25	10	65	354	387	405	33	6.44

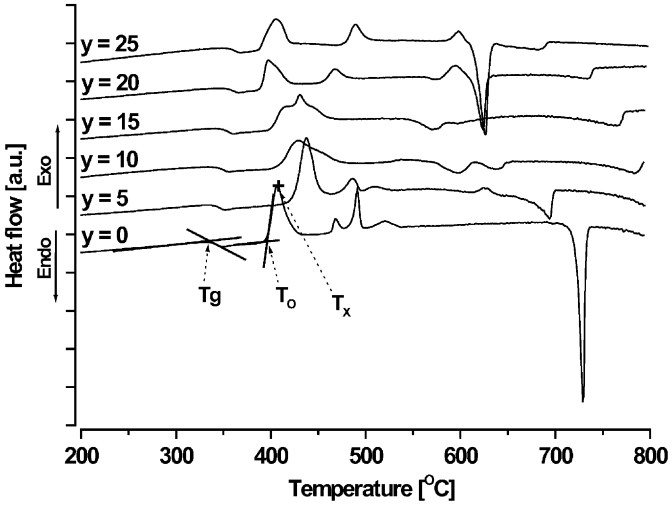

Fig. 2. DSC curves of the $yBiO_{1.5}$–$10TiO_2$–$(90-y)TeO_2$ glasses ($0 \leqslant y \leqslant 25$; heating rate 10 °C/min).

Fig. 2. (The coefficients in the formula representing various glass compositions will be given in mol% throughout this paper.) The thermal stability of the glasses was calculated as the difference in the first crystallization onset (T_o) and the glass transition temperature (T_g). All the glasses were homogeneous and yellow. It is worth noting that (i) these data were obtained from glasses prepared under the same ice-quenching conditions in order to give us comparable results; (ii) strictly the similar characteristics were measured, when it was possible, from glassy samples elaborated under air-quenching conditions.

Thus, it was found that the T_g value increases with increasing concentration of both TiO_2 and Bi_2O_3. The thermal stability of the glasses (difference T_o-T_g) changes with the composition and reaches a maximum of 86.7 °C for the $5BiO_{1.5}$–$10TiO_2$–$85TeO_2$ glass. Increasing Bi_2O_3 amount augments the densities of the glasses, and increasing amount of TiO_2 lowers their densities.

3.3. Raman spectra

The Raman spectra were considered as a source of an information about structural properties of the glasses and their composition dependences. First the study was performed for the $xTiO_2$–$(100-x)TeO_2$ system in interval between $x = 0$ and 18. The spectra of such glasses and of the related crystalline compounds with $x = 0$ (α-TeO_2), $x = 25$ ($TiTe_3O_8$) and $x = 100$ (TiO_2 rutile) are shown in Fig. 3.

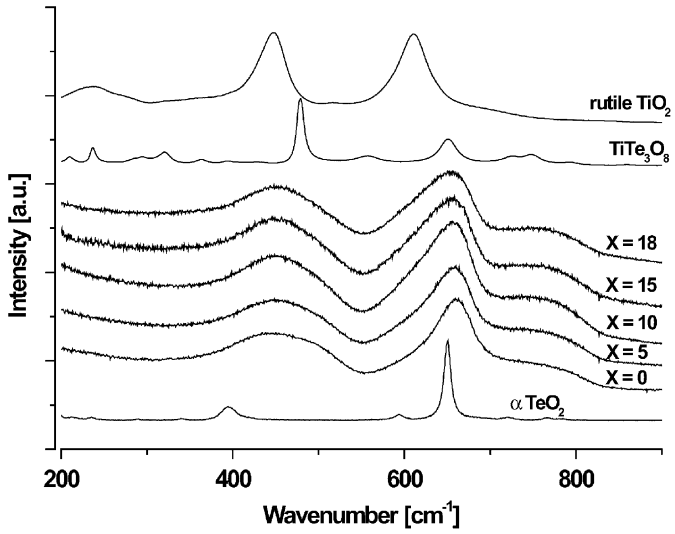

Fig. 3. Raman spectra of the $x\mathrm{TiO_2}$–$(100-x)\mathrm{TeO_2}$ glasses, and of the α-$\mathrm{TeO_2}$, $\mathrm{TiTe_3O_8}$ and $\mathrm{TiO_2}$ crystalline lattices.

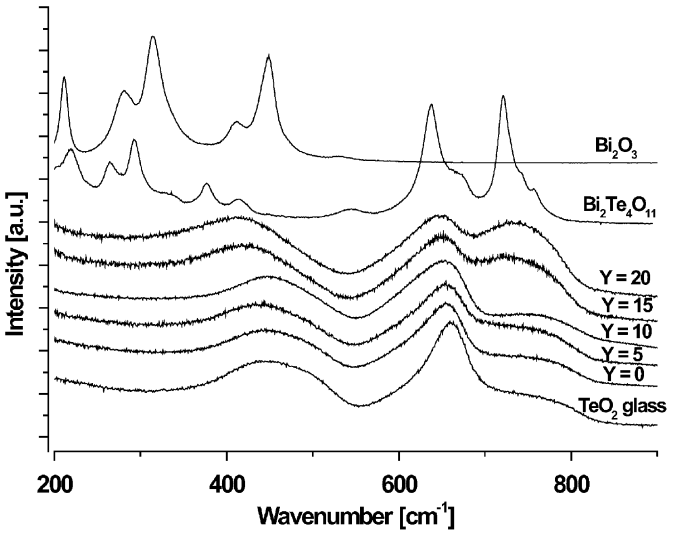

Fig. 4. Raman spectra of the $y\mathrm{BiO_{1.5}}$–$5\mathrm{TiO_2}$–$(95-y)\mathrm{TeO_2}$ glasses, comparing to the spectra of pure $\mathrm{TeO_2}$ glass and of the $\mathrm{Bi_2Te_4O_{11}}$ and $\mathrm{Bi_2O_3}$ crystalline lattices.

Then we studied the Raman spectra of the glasses within the ternary $y\mathrm{BiO_{1.5}}$–$x\mathrm{TiO_2}$–$(100-x-y)\mathrm{TeO_2}$ system in varying y, and keeping $x = 5$, 10 and 15. The results are given in Figs. 4 and 5, respectively, jointly with the spectra of the crystalline structures $\mathrm{Bi_2Te_4O_{11}}$ and $\mathrm{Bi_2O_3}$ (The spectra for $x = 15$ have coincided practically with those for $x = 10$, and therefore are not presented here).

To characterize quantitatively the evolution of the bands observed in the spectra of glasses in Figs. 3–5, their baseline corrections and decompositions into the Gaussian-like oscillators, A–D, were made and presented in Fig. 6(a)–(e) in which, "by definition", (see caption to Fig. 6) oscillator C keeps its intensity.

Figs. 3 and 6(a)–(c) show that:

(i) the original (non-baseline-corrected) spectra of the $x\mathrm{TiO_2}$–$(100-x)\mathrm{TeO_2}$ glasses in Fig. 3 demonstrate no distinct changes with increasing x;
(ii) oscillator A dominating the large band 400–500 $\mathrm{cm^{-1}}$ augments its frequency and relative intensity, and oscillator B seems to become weaker;
(iii) the highest frequency part of the spectra i.e. oscillators C and D, remains practically intact.

Figs. 4–6(b), (d), (e) show that with increasing content of $\mathrm{Bi_2O_3}$, the following three main points can be stated regarding the spectra of the $y\mathrm{BiO_{1.5}}$–$x\mathrm{TiO_2}$–$(100-x-y)\mathrm{TeO_2}$ glasses:

(iv) oscillator A displaces from 438 $\mathrm{cm^{-1}}$ [Fig. 6(b)] to 415 $\mathrm{cm^{-1}}$ [Fig. 6(e)], and becomes stronger;
(v) oscillator B progressively losses its intensity and vanishes at $y = 0.18$;
(vi) the frequency of oscillator D drops, whereas its intensity progressively augments and becomes equal to that of oscillator C for $y = 0.18$.

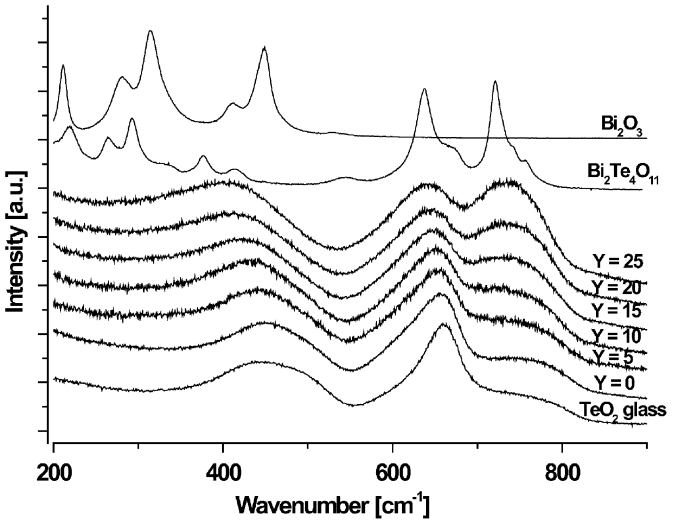

Fig. 5. Raman spectra of the $y\mathrm{BiO_{1.5}}$–$10\mathrm{TiO_2}$–$(90-y)\mathrm{TeO_2}$ glasses, comparing to the spectra of pure $\mathrm{TeO_2}$ glass and of the $\mathrm{Bi_2Te_4O_{11}}$ and $\mathrm{Bi_2O_3}$ crystalline lattices.

4. Discussion

Before discussing the relations between Raman spectra and structural properties of the binary and ternary *glassy systems*, we wish to touch on some peculiarities of the spectra and chemical bonding in pure $\mathrm{TeO_2}$ glass and in the two crystalline lattices, $\mathrm{TiTe_3O_8}$ [14] and $\mathrm{Bi_2Te_4O_{11}}$ [18] which are related to the two modifiers used in our studies. Thus, we would like to underline principal differences between the constitutions of those lattices by analysing the structures of those (Figs. 7 and 8) jointly with the relevant Raman spectra (Figs. 3–6) with the aim to extend our results into the field of the relevant binary and ternary glasses.

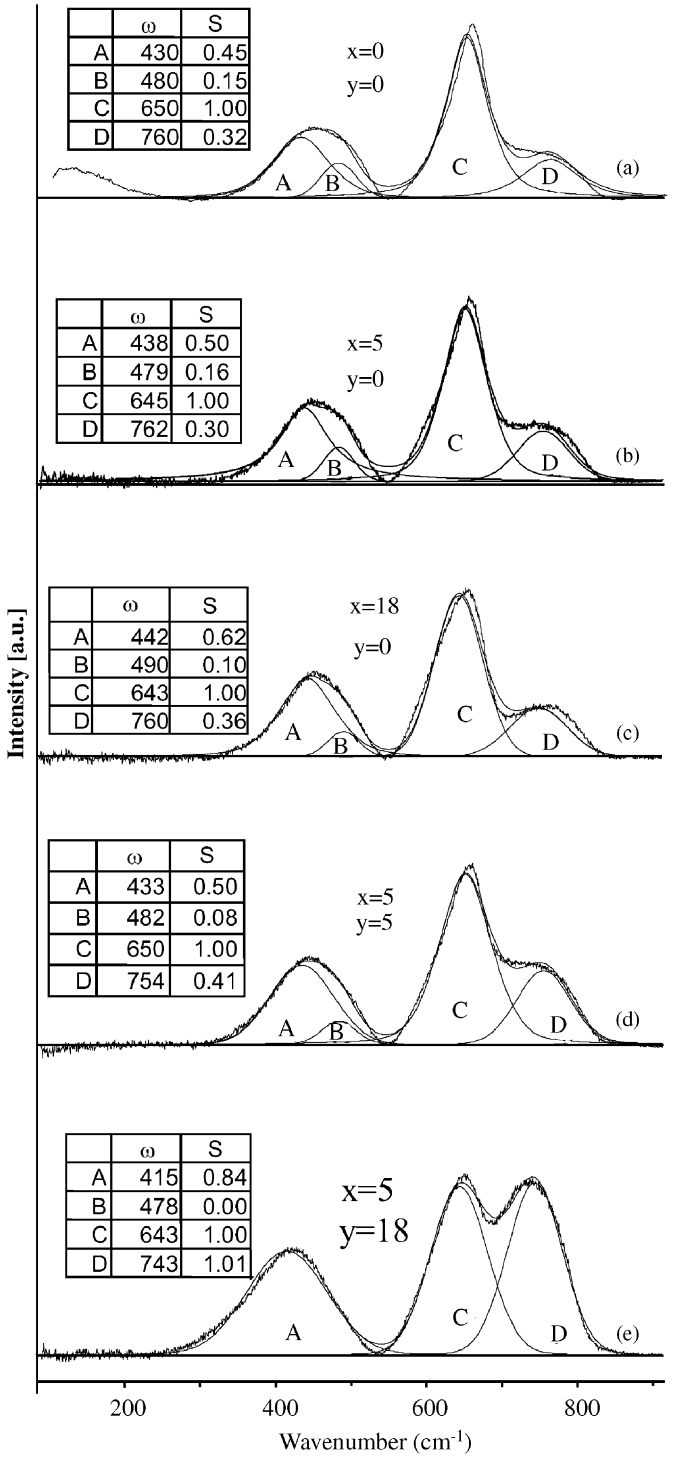

Fig. 6. Decomposition of baseline-corrected Raman spectra of some glasses of the $y\mathrm{BiO}_{1.5}$–$x\mathrm{TiO}_2$–$(100-x-y)\mathrm{TeO}_2$ composition (using the Gaussian-like oscillators, A–D). The insets show the oscillators characteristics: frequencies expressed in wavenumbers ω, and areas S normalized with respect to the area of oscillator C which is always kept equal to 1.

The Raman spectrum of pure TeO_2 glass is known for years [1]. Its interpretation justified by model calculations has been recently given in [19]. The main structural hypothesis which can be deduced from this is that TeO_2 glass is a framework made of *chain-like fragments* in which

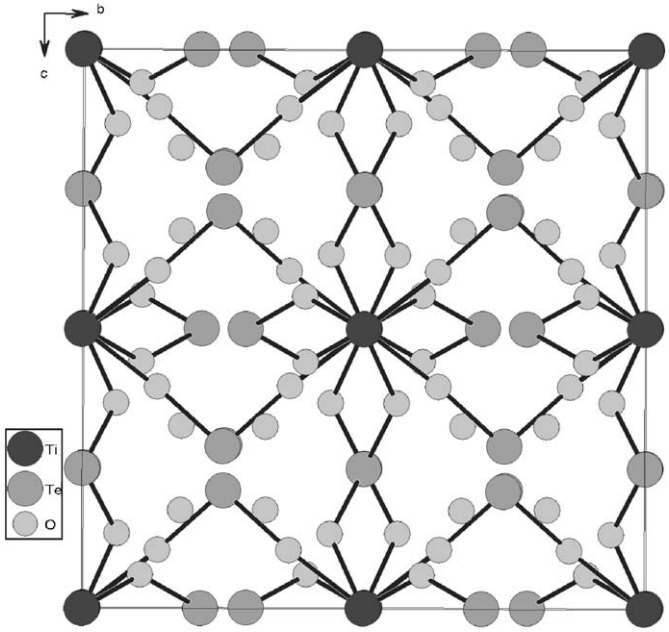

Fig. 7. Projection of the cubic cell of the $TiTe_3O_8$ crystal lattice (space group $Ia-3$) on the (010) plan. Each black circle corresponds to two Ti atoms having coinciding projections, which accounts for the doubling coordination numbers regarding to oxygen atoms. The same can be said about Te atoms in (x, 0.5, 0.25) and (x, 0.5, 0.75) positions. Only interatomic bonds shorter than 2 Å are marked.

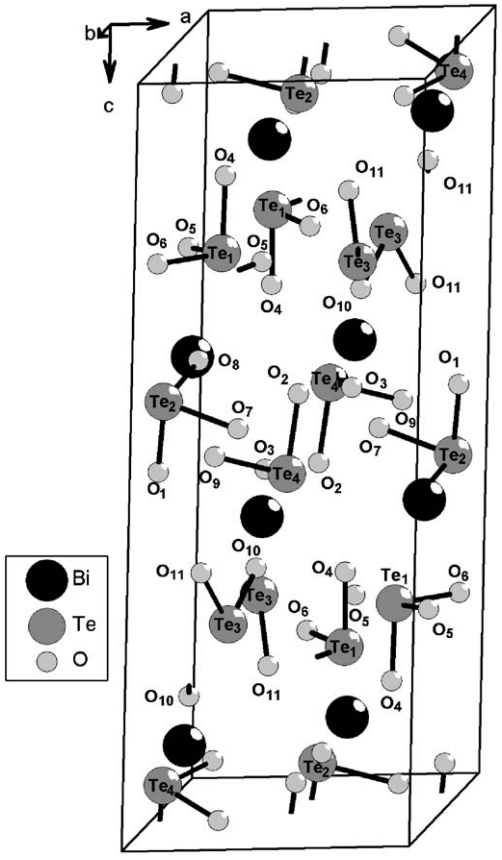

Fig. 8. Perspective view of the $Bi_2Te_4O_{11}$ unit cell (space group $P12_1/n1$). Only interatomic bonds shorter than 2 Å are marked.

the TeO_2 units are well polymerized, thus forming strong (mainly covalent) and rather symmetric Te–O–Te *intra-chain* bridges in which both the Te–O bonds have lengths of about 2.0 Å. Such bridges are typical neither for the complex tellurite anions, nor for the pure TeO_2 lattices (see α- and β-TeO_2 structures [19,20]), with the exception of γ-TeO_2 [21]. Symmetric stretchings vibrations of those bridges give rise to a large and intense band situated near 430 cm^{-1} (see the spectrum of TeO_2 glass in Fig. 3), described as oscillator A in Fig. 6(a), whereas the asymmetric stretchings have weak intensities and are localized above 700 cm^{-1} (oscillator D). The inter-chain linkages are realised via "standard" Te–O–Te bridges [i.e., those which are formed by the so-called axial bonds (having 2.10–2.15 Å in length) and equatorial bonds (1.85–1.90 Å) similar to the Te–O–Te linkages in the α- and β-TeO_2 lattices as well as in many tellurite structures], whose symmetric and asymmetric vibrations are situated near 480 cm^{-1} [oscillator B in Fig. 6(a)] and near 660 cm^{-1} [oscillator C in Fig. 6(a)], respectively.

The Raman spectrum of crystalline $TiTe_3O_8$ (Fig. 3) is dominated by a relatively strong band near 440 cm^{-1} and a weaker band near 650 cm^{-1} (a high frequency part of the infrared spectrum of this lattice can be found in Ref. [16]). It must be particularly underlined that the absence of strong bands in the high-frequency (stretching) region of the spectrum shows that this structure is a framework [15] in which neither Ti–O bonds, nor Te–O bonds can be considered as terminal ones, but forming the covalently bonded Te–O–Ti bridges. Therefore, the interpretation of those bands in terms of localized Ti–O or Te–O bond vibrations is unambiguous: actually, they correspond to the motions of oxygen atoms in the potential wells formed by the Te–O–Ti linkages (Fig. 7).

Moreover, we venture the opinion, that from the formal chemical point of view, the $TiTe_3O_8$ lattice cannot be considered as a tellurite structure: actually, neither simple $[TeO_3]^{2-}$ *ortho*-anions, nor complex $[Te_3O_8]^{4-}$ anions exist there (see Fig. 7) in contrast to structures like $Zn_2Te_3O_8$, in which such complex anions are the fundamental structural units [16]. So it can be specified as a crystalline phase of the $25TiO_2$–$75TeO_2$ "*solid solution*" of TiO_2 in TeO_2. In addition, we wish to remark that the resemblance of the band positions in the spectra of pure TeO_2 glass and of $TiTe_3O_8$ structures (Fig. 3) is dictated by the resemblance of the chemical nature of the binding between the oxygen atoms and their nearest neighbours, and, correspondingly, of the lengths of the bonds forming the Te–O–Te and Ti–O–Te bridges in those structures, respectively.

The spectrum of the $Bi_2Te_4O_{11}$ lattice [Figs. 4 and 5] reflects a significant difference between its chemical constitution and that of the $TiTe_3O_8$ lattice. Actually, while no $[Te_nO_m]^{2(m-2n)-}$ tellurite anions are present in the latter structure (Fig. 7), the $[Te_4O_{11}]^{6-}$ anions can be readily recognized in the former (Fig. 8). According to a schema proposed in [10], those complex anions can be regarded as framed of the four dipole structural blocks: three *ortho*-ions $[TeO_3]^{2-}$ (see coordination polyhedrons around atoms Te1, Te2 and Te4 in Fig. 8) and one molecule TeO_2 in which Te atom has two complementary neighbouring oxygen atoms, thus forming a so-called disphenoid (see the coordination polyhedron around atom Te3 which forms two strong "molecular" bonds with atoms O11 and O10, and two much weaker contacts with atoms O6 and O5). Thus, the strong Te–O–Te bridges are absent in this structure.

Consequently, in its Raman spectrum (Figs. 4 and 5), the area between 400 and 500 cm^{-1} is practically empty, whereas the two strong lines are present above 600 cm^{-1}. The highest of them (near 720 cm^{-1}) has a position and an intensity characteristic for the synchronous pulsation vibrations of the terminal bonds in the $[TeO_3]^{2-}$ units [20,22]. The second band (645 cm^{-1}) can be attributed to the symmetric stretching vibrations of the TeO_2 molecules in condensed mediums (see e.g. [10,19]). As for the two bands around 400 cm^{-1}, our lattice dynamical calculations show that they are associated with Te–O–Bi linkages.

It is still worth underlining that the absence of intense lines between 400 and 500 cm^{-1} in the spectrum just indicates that the neutral TeO_2 molecules and the charged $[TeO_3]^{2-}$ pyramids form the $[Te_4O_{11}]^{6-}$ complex tellurite anions without polymerizing via the Te–O–Te linkage. According to the Raman spectroscopy data, such a situation seems to be customary for complex tellurite structures (e.g. Refs. [10,22]).

In line with this, the evolution of TeO_2 glass into a tellurite structure is associated, as a rule, with depolymerization effects because of which the large and intense band 400–500 cm^{-1} inherent in the spectrum of pure TeO_2 glass eventually disappears. During this evolution, the formation of the $[TeO_3]^{2-}$ *ortho*-anions gives rise to a strong Raman-active band near 720–730 cm^{-1}, whereas the TeO_2 molecules which rest "intact" manifest themselves by the band near 650 cm^{-1}. Therefore, it can be said that the high-frequency part of the Raman spectrum of the $Bi_2Te_4O_{11}$ lattice has the features of "classic" spectra of the $[Te_nO_m]^{2(m-2n)-}$ complex tellurite anions which are discussed in [10,15].

4.1. $xTiO_2$–$(100-x)TeO_2$ glasses

The lowering glass density (over all the glass forming domain from 5 to 18 mol% of TiO_2) with increasing x can be naturally associated with the contribution of relatively lightweight atoms of titanium. The densities of obtained glasses are quite comparable to those previously reported in literature [23].

The main features of the structural evolution of the $xTiO_2$–$(100-x)TeO_2$ glasses at increasing x should be deduced from the interpretation of the changes in the spectra in Figs. 3 and 6(a)–(c), i.e., from the explication of the items (i)–(iii) indicated in Section 3.3.

First, we concern with the item (i). The absence of the bands related to pure titanium dioxide framework

(characterized by the three-fold coordination of atoms of oxygen) in the spectra of the $x\mathrm{TiO_2}$–$(100-x)$ glassy samples (see Fig. 3) allows us to think that those are monophase systems in which TiO_6 polyhedrons are interconnected via $TeO_{4/2}$ disphenoids like in the $TiTe_3O_8$ lattice. This implies the existence of the two types of bridges in those glasses: Te–O–Ti and Te–O–Te bridges. The former bridges would manifest their presence in the spectra by bands similar to those observed for $TiTe_3O_8$. However, positions and relatively weak intensities of those bands (see Fig. 3) cannot influence dramatically the initial shape of the spectrum (i.e. that of pure TeO_2 glass), which can account for point (i).

Now we concentrate on the items (ii) and (iii). Note first that the peculiarities of the evolution of spectra indicated there resemble those observed in the Raman spectra of pure TeO_2 during its glass–liquid transformation [19] at heating. A vanishing of the weak shoulder of the band 400–500 cm^{-1} simultaneously with the strengthening of the wing above 700 cm^{-1} (see Fig. 4 in [19]), was interpreted as indication of the breaking of the *inter-chain* bridges in TeO_2 at melting leading to the appearance of the Te–O terminal bonds in the liquid.

The similar idea comes in mind when analysing the spectra in Figs. 3 and 6(a)–(c). Reasoning from the above-mentioned peculiarities of the crystal chemistry of the $TiTe_3O_8$ lattice, we are led to conclude that the glass structures within the $x\mathrm{TiO_2}$–$(100-x)\mathrm{TeO_2}$ system can be specified in terms of solid solutions of TiO_2 in TeO_2, as it was proposed above for the $TiTe_3O_8$ crystalline lattice.

Actually, the formation of those glasses with increasing x would change the coordination polyhedrons neither around Ti atom nor around Te atom, and would result in the following alterations: (a) the disappearance of the "standard" inter-chain Te–O–Te linkages (leading to a decay of oscillator B), which are weak since they involve the weak axial Te–O bonds (about 2.15 Å in length); (b) the formation of stronger Te–O–Ti bridges (made of two relatively strong bonds having 1.95 Å in length) replacing just mentioned Te–O–Te linkages. These account for the items (ii) and (iii), respectively.

The fact of such a transformation is indirectly confirmed by our another observations: glass transition temperature T_g increases with increasing TiO_2 content, thus indicating the substitution of the Te–O–Te bridges inherent of pure TeO_2 by the stronger chemical linkages Te–O–Ti. In general, our interpretation of the experimental data is in line with results early obtained by Sabadel et al. [3,11,12].

4.2. Bi_2O_3–TiO_2–TeO_2 glasses

Under ice-quenching conditions, the glass forming domain for the Bi_2O_3–TeO_2 binary system extends in a very narrow range of composition (only up to ~4 mol% of $BiO_{1.5}$). However, the addition to this system of the third component, TiO_2, results in a broad glass domain extending in some cases up to 25 mol% of $BiO_{1.5}$ (Fig. 1). Within this ternary system, for a fixed concentration of TiO_2, the increasing content of Bi_2O_3 provides a practically linear increase of glass densities which is readily explained by the very high molecular weight of the latter oxide.

We focus now on the evolution of the spectra in Figs. 4–6(b), (d), (e) with the aim to comment the items (iv)–(vi) in Section 3.3 in terms of the structural changes in the Bi_2O_3–TiO_2–TeO_2 glasses. A sharp strengthening of the oscillator D which lowers its position with increasing y [see Fig. 6(b), (d), (e)] indicates beyond any reasonable doubt that an increasing number of $[TeO_3]^{2-}$ *ortho*-groups are formed in the glasses, and the latter evaluate to a "classic" tellurite structures with complex anions resembling those in the $Bi_2Te_4O_{11}$ lattice. In other words, an increasing modifier (Bi_2O_3) content provokes a "normal" progressive transformation of the TeO_2 glass network into a typic tellurite structure, i.e., into an ensemble of alternate complex tellurite anions and monoatomic cations.

The evolution of the band occupying interval between 400 and 500 cm^{-1} (items iv and v), is in line with the above conclusion. Actually, its shift towards 400 cm^{-1} just indicates a decay of the initial framework ($y = 0$) and its depolymerization with increasing y, i.e. the replacement of the strong Te–O–Te and Te–O–Ti bridges by weaker Te–O–Bi linkages which were discussed above, when considering the spectrum of crystalline $Bi_2Te_4O_{11}$. It can be added, that, theoretically, the formation of any $y\mathrm{BiO_{1.5}}$–$x\mathrm{TiO_2}$–$(100-x-y)\mathrm{TeO_2}$ glass structure implies a possibility for appearance of another types of bridges like Ti–O–Ti, Bi–O–Bi and Ti–O–Bi, but none of them can be "revealed" from the spectra.

We note that the transformation of glassy TeO_2 network induced by an addition of modifiers with cations having a valence of one or two, as a rule, reduces the T_g values [1]. Therefore, it is important to underline that the T_g values of our glasses always increases with the progressive additions of TiO_2 or Bi_2O_3. Thus, it can be suggested that the substitution of the Te–O–Te bridges by new Te–O–M bridges in which the M-elements have valences of three, four and higher, would augment thermal and mechanical resistance of tellurite glasses, whether they are of framework-type or not.

5. Summary and conclusions

A glass forming domain was evidenced in the $y\mathrm{BiO_{1.5}}$–$x\mathrm{TiO_2}$–$(100-x-y)\mathrm{TeO_2}$ system, but no glass formation was observed in the $y\mathrm{BiO_{1.5}}$–$x\mathrm{ZrO_2}$–$(100-x-y)\mathrm{TeO_2}$ system. For $y = 0$, the evolution of the Raman spectra of the TiO_2–TeO_2 glasses at increasing TiO_2 content allows us to conclude that no tellurite anions are built up in that structure, and the Te–O–Te linkages are progressively substituted by Te–O–Ti, due to which the framework arrangement of the glass is kept. In contrast to this, the addition of Bi_2O_3 results in breaking off the initial glass framework, thus provoking its depolymerization, and in forming local complex tellurite anions interconnected via

atoms of Bi. The increase of the T_g values observed in both the cases indicates a relative strength of the Ti–O–Te and Bi–O–Te bridges replacing the Te–O–Te ones.

Acknowledgments

Three of us, M. Udovic, O. Durand and M. Soulis are grateful to the Conseil Régional du Limousin for financial support.

References

[1] R.A.F. El-Mallawany, Tellurite Glasses Handbook: Properties and Data, CRC Press, Boca Raton, FL, 2002.
[2] K. Sae-Hoon, T. Yoko, J. Am. Ceram. Soc. 78 (4) (1995) 1061–1065.
[3] J.C. Sabadel, P. Armand, D. Cachau-Hereillat, P. Baldeck, O. Foclot, A. Ibanez, E. Philippot, J. Solid State Chem. 132 (1997) 411–419.
[4] S. Le Boiteux, P. Segonds, L. Canioni, L. Sarger, E. Fargin, T. Cardinal, C. Duchesne, G. Le Flem, J. Appl. Phys. 81 (1997) 1481–1487.
[5] B. Jeansannetas, S. Blanchandin, P. Thomas, P. Marchet, J.C. Champarnaud-Mesjard, T. Merle-Méjean, B. Frit, V. Nazabal, E. Fargin, G. Le Flem, M.O. Martin, B. Bousquet, L. Canioni, S. Le Boiteux, P. Segonds, L. Sarger, J. Solid State Chem. 146 (1999) 329–335.
[6] J. Lin, W. Huang, Z. Sun, C.S. Ray, D.E. Day, J. Non-Cryst. Solids 336 (2004) 189–194.
[7] O. Noguera, M. Smirnov, A.P. Mirgorodsky, T. Merle-Méjean, P. Thomas, J.C. Champarnaud-Mesjard, J. Non-Cryst. Solids 345&346 (2004) 734–737.
[8] O. Noguera, M. Smirnov, A.P. Mirgorodsky, T. Merle-Méjean, P. Thomas, J.C. Champarnaud-Mesjard, Phys. Rev. B 68 (2003) 094203/1–094203/10.
[9] A.P. Mirgorodsky, M. Smirnov, M. Soulis, P. Thomas, T. Merle-Méjean, Phys. Rev. B 73 (2006) 134206/1–134206/13.
[10] O. Noguera, T. Merle-Méjean, A.P. Mirgorodsky, P. Thomas, J.C. Champarnaud-Mesjard, J. Phys. Chem. Solids 65 (2004) 981–993.
[11] J.C. Sabadel, P. Armand, P.E. Lippens, D. Cachau-Herreilat, E. Philippot, J. Non-Cryst. Solids 244 (1999) 143–150.
[12] J.C. Sabadel, P. Armand, F. Terki, J. Pelous, D. Cachau-Herreilat, E. Philippot, J. Phys. Chem. Solids 61 (2000) 1745–1750.
[13] J.C. Sabadel, P. Armand, E. Philippot, Phys. Chem. Glasses 41 (1) (2000) 17–23.
[14] G. Meunier, J. Galy, Acta Crystallogr. B 27 (1971) 602–608.
[15] O. Noguera, Thesis of the University, No. 48-1999, Limoges, November 2004.
[16] M. Arnaudov, V. Dimitrov, Y. Dimitriev, L. Markova, Mater. Res. Bull. 17 (1982) 1121–1129.
[17] T. Sekiya, M. Mochida, A. Soejima, J. Non-Cryst. Solids 191 (1995) 115–123.
[18] H.J. Rossel, M. Leblanc, G. Férey, D.J.M. Bevan, D.J. Simpson, M.R. Taylor, Aust. J. Chem. 45 (1992) 1415–1425.
[19] O. Noguera, T. Merle-Méjean, A.P. Mirgorodsky, M. Smirnov, P. Thomas, J.C. Champarnaud-Mesjard, J. Non-Cryst. Solids 330 (2003) 50–60.
[20] A.P. Mirgorodsky, T. Merle-Méjean, J.C. Champarnaud-Mesjard, P. Thomas, B. Frit, J. Phys. Chem. Solids 61 (2000) 501–509.
[21] J.C. Champarnaud-Mesjard, S. Blanchandin, P. Thomas, A.P. Mirgorodsky, T. Merle-Méjean, B. Frit, J. Phys. Chem. Solids 61 (2000) 1499–1507.
[22] T. Sekiya, M. Mochida, A. Ohtsuka, M. Tonokawa, J. Non-Cryst. Solids 144 (1992) 128–144.
[23] V. Dimitrov, T. Komatsu, J. Non-Cryst. Solids 249 (1999) 160–179.